

# Importance of the singular constitutive parameters of cylindrical cloaks : illustration on the anticloak concept

Blanchard, Cédric; Zhang, Baile; Wu, Bae-lan; Portí, Jorge Andrés; Chen, Hongsheng; Morente, Juan Antonio; Salinas, Alfonso

2009

Blanchard, C., Zhang, B., Wu, B. I., Portí, J. A., Chen, H., Morente, J. A., et al. (2009). Importance of the singular constitutive parameters of cylindrical cloaks: illustration on the anticloak concept. *Journal of the Optical Society of America B*, 26(9), 1831-1836.

<https://hdl.handle.net/10356/95036>

<https://doi.org/10.1364/JOSAB.26.001831>

---

© 2009 OSA. This paper was published in *Journal of the Optical Society of America B* and is made available as an electronic reprint (preprint) with permission of Optical Society of America. The paper can be found at: [DOI: <http://dx.doi.org/10.1364/JOSAB.26.001831>]. One print or electronic copy may be made for personal use only. Systematic or multiple reproduction, distribution to multiple locations via electronic or other means, duplication of any material in this paper for a fee or for commercial purposes, or modification of the content of the paper is prohibited and is subject to penalties under law.

*Downloaded on 09 Apr 2024 16:24:15 SGT*

# Importance of the singular constitutive parameters of cylindrical cloaks: illustration on the anticloak concept

Cédric Blanchard,<sup>1,2,\*</sup> Baile Zhang,<sup>2</sup> Bae-Ian Wu,<sup>2</sup> Jorge Andrés Portí,<sup>1</sup> Hongsheng Chen,<sup>2,3</sup> Juan Antonio Morente,<sup>1</sup> and Alfonso Salinas<sup>1</sup>

<sup>1</sup>Department of Applied Physics, University of Granada, 18071 Granada, Spain

<sup>2</sup>Research Laboratory of Electronics, Massachusetts Institute of Technology, Cambridge, Massachusetts 02139, USA

<sup>3</sup>The Electromagnetics Academy at Zhejiang University, Zhejiang University, Hangzhou 310027, China

\*Corresponding author: cedric@ugr.es

Received April 23, 2009; accepted June 26, 2009;  
posted August 6, 2009 (Doc. ID 110411); published August 31, 2009

Two-dimensional electromagnetic cloaking devices with infinite optic constants at the inner boundary are investigated. Numerical simulations of this class of ideal cloak, performed with the transmission line modeling method, confirm the fundamental importance of such extreme values in the efficiency of the cloak in some situations. This is illustrated by using the concept of the anticloak, which was shown to be capable of defeating the non-ideal cloak. We numerically show that the presence of a layer with extreme constitutive parameters renders the anticloak unable to produce its effect. Furthermore, we propose a simple theoretical model that leads to the same conclusion if the cloak is slightly dissipative. © 2009 Optical Society of America

OCIS codes: 230.3205, 050.1755, 160.3918.

## 1. INTRODUCTION

Invisibility cloaking has recently been under intense study since the pioneering work proposed by Pendry *et al.* [1]. Experimental realization [2] as well as many theoretical developments [3–10] backed up by numerical modeling [11–14] have allowed significant progress on this topic.

An issue of great concern to physicists is whether the cloaking effect can be achieved under any condition. In this sense, it has been shown that the ideal two-dimensional cloak is very sensitive to the slightest perturbation [5]. Still, for the cylindrical case it has been established that extending the inner boundary of the cloaking shell toward the concealed region appears to allow further penetration of the field [6]. Nonetheless, the effectiveness of the cloaking was not questioned in [6] since the power cannot go into the cloak. It should be emphasized that [5,6] clearly stressed the fundamental role of the extreme inner layer for which the azimuth permittivity or permeability (depending on the electromagnetic polarization under consideration) are infinite while the other electromagnetic parameters are zero. Furthermore, it has been more recently proven that a certain kind of anisotropic material located beyond the inner boundary of the cloak can cancel out the cloaking effect [15,16]. The permittivity,  $\epsilon$ , and permeability,  $\mu$ , of such an anticloak are derived using a coordinate transformation whose slope is negative compared to the original one; the electromagnetic space associated with the cloak is then reconstructed by the anticloak, rendering the object inside the anticloak visible [15]. It is interesting to note that there are two sets of solutions to Maxwell's equations in this case. One dictates

that the field cannot penetrate into the cloak irrespective of what is inside [5,6], while the other shows that the field can penetrate into the cloaked region by virtue of the anticloak [15]. However, it is arduous to verify this extreme case for which both the cloak and the anticloak exist and interact with each other. The analytic calculations in [5,6] did not consider the possibility of including such an anisotropic anticloak, while [15] used a nonzero perturbation parameter that approaches the ideal case without rigorously reaching it. Therefore, the ideal situation requires further analysis, as mentioned in [15], but dealing with extreme parameters is challenging from both the analytical and computational point of view. Mathematically, when the perturbation parameter goes to zero, the transformation becomes a singular mapping, and the Jacobian matrix does not exist at the interface between the cloak and the anticloak. For this reason, cloaking modeling usually assumes upper and lower limits of constitutive parameters, while the required  $\epsilon$  or  $\mu$  span the entire range from zero to infinity.

In the present work, the singular behavior of the anticloak is studied using the transmission line modeling (TLM) method [17,18]. First, an innovative extension of TLM is developed, allowing the resolution of problems involving infinite values for  $\epsilon$  or  $\mu$ . Second, we find that when the perturbation parameter is nonzero, the anticloak can cancel the cloaking effect outside. However, when it is zero, the presence of an extreme layer between the cloak and the anticloak ensures that the cloaking effect is still achieved, irrespective of the core composition. Third, an analytical model is developed to explain this behavior.

## 2. CYLINDRICAL CLOAK AND ANTICLOAK

To be effective, the dielectric and magnetic constants of the anisotropic cloak must take specific values [1,11]. Let the inner and outer radius be represented by  $R_1$  and  $R_2$ , respectively. The simple following transformation,

$$r = (r' - R_2) \frac{R_2 - R_1}{R_2 - c} + R_2, \quad \varphi = \varphi', \quad z = z', \quad (1)$$

that can compress the space from  $0 < r' < R_2$  to the annular region  $a < r < R_2$ , yields

$$\begin{aligned} \varepsilon_r = \mu_r &= \frac{r - a}{r}, \\ \varepsilon_\varphi = \mu_\varphi &= \frac{r}{r - a}, \\ \varepsilon_z = \mu_z &= \left( \frac{R_2 - c}{R_2 - R_1} \right)^2 \frac{r - a}{r}, \end{aligned} \quad (2)$$

where  $c$  is the perturbation parameter and  $a = R_2(R_1 - c)/(R_2 - c)$ . The parameter  $c$  marks the degree of imperfection of the cloak. In this manner, a zero value of  $c$  makes  $\varepsilon$  or  $\mu$  ideal, which results in a perfect cloak.

Let  $R_0$  be a third boundary inside the cloak in such a way that  $0 < R_0 < R_1$ . In agreement with [15], the transformation

$$r = (r' - d) \frac{R_0 - R_1}{d - c} + R_0, \quad \varphi = \varphi', \quad z = z', \quad (3)$$

leads to the anticloak parameters

$$\begin{aligned} \varepsilon_r = \mu_r &= \frac{r - b}{r}, \\ \varepsilon_\varphi = \mu_\varphi &= \frac{r}{r - b}, \\ \varepsilon_z = \mu_z &= \left( \frac{d - c}{R_0 - R_1} \right)^2 \frac{r - b}{r}, \end{aligned} \quad (4)$$

where  $d$  is a constant, and  $b = (R_1 d - R_0 c)/(d - c)$ . Chen *et al.* have claimed that the parameters of Eq. (4) are capable of destroying the effect of an invisibility cloak when  $c$  is nonzero [15]. Nevertheless, our work differs from theirs in one important respect: we will consider the case in which  $c$  is strictly equal to zero, i.e.,  $(\varepsilon_\varphi, \mu_\varphi) = +\infty$  in the cloak and  $(\varepsilon_\varphi, \mu_\varphi) = -\infty$  in the anticloak at  $r = R_1$ .

## 3. TLM STUDY OF THE CLOAK/ANTICLOAK INTERACTION

In the following, we will consider that the incoming plane wave has a transverse electric (TE) polarization, i.e., with the electric field,  $E_z$ , normal to the plane of propagation. As it has been pointed out above, the achievement of ideal cloaking requires infinite values of  $\mu_\varphi$  at  $r = R_1$ . The difficulty in assuming such an infinite value is often eluded by truncating the inner layer, which leads to large but finite

values of  $\mu_\varphi$ . Often, substituting the actual infinite values by approximate finite ones is done without significant consequences. For instance, very accurate modeling of the cloaking effect can be reached if  $\mu_\varphi$  is chosen to be high enough [5,11]. However, certain studies may require this quantity to be actually infinite. It is the case of the anti-cloaking phenomenon for which no complete study can be carried out without being able to exactly consider an infinite  $\mu_\varphi$ . In this sense, TLM is well suited for the anticloak modeling given that infinite values of  $\mu_\varphi$  are of no consequence to the convergence of the method, as we show hereinafter.

TLM is a time-domain method entirely based upon establishing a relation between the physical problem to be solved and an analogous electric network. The space is filled out with a large number of nodes that are formed by appropriately connecting transmission lines. For the purpose of illustration, a two-dimensional TLM node for TE modes is depicted in Fig. 1. In order to represent cylindrical structures such as the cloak of interest here, a cylindrical mesh rather than a Cartesian mesh is preferred. This allows assumption of a cylindrical shape and thus avoids staircase approximations. The node in Fig. 1 is made up of four main lines (ports 1–4), that connect the current node with the adjacent ones. The four connecting lines all have the same characteristic impedance,  $Z_0$ , and characteristic admittance,  $Y_0 = 1/Z_0$ . The incorporation of stubs (only connected at the node center) to the node offers an independent control on permittivity, permeability, and conductivity. A capacitive stub (port 5) with admittance  $Y_z Y_0$  confers extra capacitance to the node and then allows a control on  $\varepsilon_z$ . Two inductive stubs (ports 6 and 7)

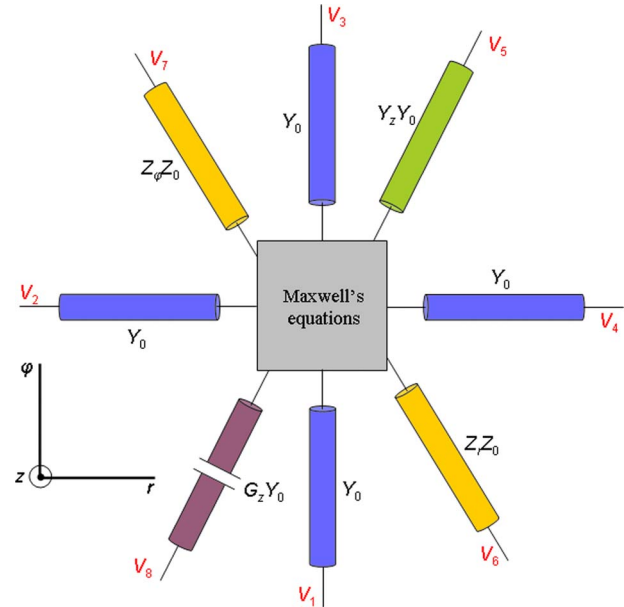


Fig. 1. (Color online) Upper view of a two-dimensional node for TE modes in cylindrical coordinates. Four link lines (with admittance  $Y_0$ ) are connected to the four adjacent nodes and allow the propagation of the pulses into the mesh. The four other stub lines are connected at the node center without being connected to any other lines; the capacitive stub (with normalized admittance  $Y_z$ ) is an open circuit; the two inductive stubs (with normalized impedance  $Z_r$  and  $Z_\varphi$ ) are short circuits; and the lossy stub (with normalized admittance  $G_z$ ) is infinite.

with impedance  $Z_r Z_0$  and  $Z_\varphi Z_0$  allow a control on  $\mu_r$  and  $\mu_\varphi$  by providing extra inductance to the node. Finally, an infinitely long stub (port 8) with admittance  $G_z Y_0$  accounts for the electric conductivity  $\sigma_z$ ; note that any pulse scattered into the infinite lossy stub does not have the possibility to return. The global node in Fig. 1 can be split into three subnodes, each one representing a component of the Maxwell's equations [19]. It is worth mentioning that two supplementary infinite stubs could be added to the node to describe magnetic losses, but since no magnetic losses are present in the structure under consideration, they will not be included to rule out an unnecessary increase in the computational requirements. The mesh is then solved by evaluating the voltage pulses (numerical equivalent of the electromagnetic wave in TLM) that propagate within it. When reaching the center of the nodes, the voltage pulses are scattered according to a scattering matrix,  $\mathbf{S}$ , we give hereinafter. Finally, metamaterials are easily modeled by inverting the capacitive and inductive stubs of the node [20,21]. While the scattering matrix presented in [21] was expressed in Cartesian coordinates, use of cylindrical coordinates in the present work leads to a new expression:

$$\mathbf{S} = \begin{bmatrix} a_r & c & b_r & c & g & -i_r & 0 \\ c & a_\varphi & c & b_\varphi & g & 0 & i_\varphi \\ b_r & c & a_r & c & g & i_r & 0 \\ c & b_\varphi & c & a_\varphi & g & 0 & -i_\varphi \\ c & c & c & c & f & 0 & 0 \\ -e_r & 0 & e_r & 0 & 0 & h_r & 0 \\ 0 & e_\varphi & 0 & -e_\varphi & 0 & 0 & h_\varphi \end{bmatrix}. \quad (5)$$

Note that the node is made up of a total of 8 lines that should lead to an  $8 \times 8$  matrix. However, as no incident voltages are coming from the lossy stubs,  $\mathbf{S}$  can be reduced to a matrix of 7 columns by 8 rows. Moreover, the pulses that are reflected from the node center to the lossy stubs are usually not of valuable interest, and  $\mathbf{S}$  can consequently be reduced to a  $7 \times 7$  matrix. The elements of the matrix depend on the normalized impedances and admittances of the stubs,

$$\begin{aligned} Z_r &= \frac{2\mu_r \mu_0 r \Delta \varphi \Delta z}{Z_0 \Delta t \Delta r} - 2, \\ Z_\varphi &= \frac{2\mu_\varphi \mu_0 \Delta r \Delta z}{Z_0 \Delta t r \Delta \varphi} - 2, \\ Y_z &= \frac{2\varepsilon_z \varepsilon_0 r \Delta \varphi \Delta r}{Y_0 \Delta t \Delta z} - 4, \end{aligned} \quad (6)$$

according to

$$\begin{aligned} a_k &= \frac{2}{4 + Y_z + G_z} - \frac{2}{2 + Z_k}, \quad f = \frac{Y_z - G_z - 4}{Y_z + G_z + 4}, \\ b_k &= \frac{2}{4 + Y_z + G_z} - \frac{Z_k}{2 + Z_k}, \quad g = \frac{2Y_z}{4 + Y_z + G_z}, \end{aligned}$$

$$c = \frac{2}{4 + Y_z + G_z}, \quad h_k = \frac{2 - Z_k}{2 + Z_k},$$

$$e_k = \frac{2Z_k}{2 + Z_k}, \quad i_k = \frac{2}{2 + Z_k}, \quad (7)$$

with  $k = \{r, \varphi\}$ . In Eq. (6),  $r$  is the radial coordinate;  $\Delta r$ ,  $\Delta \varphi$ , and  $\Delta z$ , are the size of the nodes along each direction; and  $\Delta t$  is the TLM time step. It is plain from Eq. (6) that  $\mu_\varphi$  tending to infinity results in  $Z_\varphi$  becoming infinite as well. Consideration of Eq. (7) indicates that  $a_\varphi$ ,  $b_\varphi$ ,  $e_\varphi$ ,  $h_\varphi$ , and  $i_\varphi$  all remain finite for such an extreme value of the inductive stub, which leads to the conclusion that optic constants that rigorously tend to infinity are acceptable with TLM. In this manner, with regard to our actual concern, the limit  $c$  being strictly zero can be reached.

Let us now consider a cylindrical cloaking structure surrounded by free space and illuminated by a monochromatic TE electromagnetic plane wave whose frequency is 2 GHz. The cloaking shell has an inner radius  $R_1 = 0.1$  m, while the outer radius is  $R_2 = 0.2$  m. From 0 to  $R_0 = 0.05$  m, the space is occupied by a perfectly electric conducting (PEC) cylinder. Then, from  $R_0$  to  $R_2$ , different cases are envisaged and the results are depicted in Fig. 2.

(a) From  $R_0$  to  $R_1$  there is free space, and from  $R_1$  to  $R_2$  we use the cloaking parameters of Eq. (2) with  $c = 0.001$  m and  $d = 0.02$  m. The computed electric field mapping is presented in Fig. 2(a). Although we are in a nonideal situation, mainly due to the lack of extreme values at  $r = R_1$ , the cloaking effect can be achieved.

(b) From  $R_0$  to  $R_1$  the anticloak parameters of Eq. (4) are used, while Eq. (2) is used for the cloaking shell from  $R_1$  to  $R_2$ . In both case,  $c$  and  $d$  are still equal to 0.001 and 0.02, respectively. The result shown in Fig. 2(b) demonstrates that the anticloak destroys the cloaking effect observed in Fig. 2(a).

(c) The modeling differs from the previous one in one fundamental point:  $c = 0$ , i.e., the parameters of Eqs. (2) and (4) now take extreme values at  $r = R_1$ . The electric field is depicted in Fig. 2(c). The main conclusion is that the cloaking effect is no longer perturbed by the presence of the anticloak inside. Furthermore, since losses in metamaterials are unavoidable, we have incorporated a low level of electric losses to the cloak in order to make the modeling more physically realistic. It turns out that no significant deviation in the result is observed—the anticloak is still concealed by the cloak. Consequently, the lossless media that was first considered can be treated as the limit of the lossy case as the dissipation approaches zero. This indicates that the uniqueness theorem [22], stating that a field in a lossy region is unique, can be extended to the lossless media for which the theorem breaks down in general.

(d) For the sake of completion, a simple PEC cylinder with radius equal to  $d$  is modeled. The corresponding electric field mapping is shown in Fig. 2(d). As it has been pointed out in [15], the scattering is the same as in case (b).



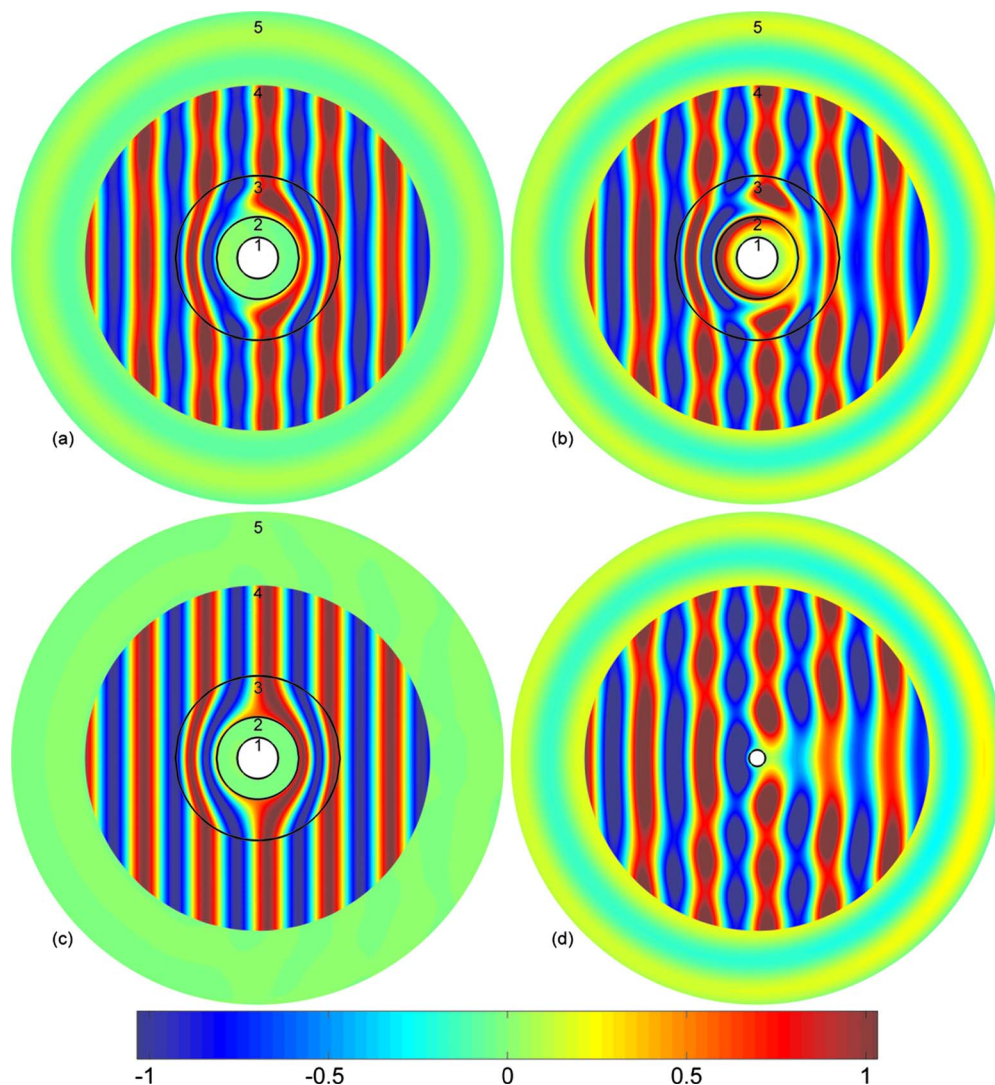


Fig. 2. (Color online) Electric field mapping for four configurations. (a) Non-ideal ( $c=0.001$ ) cloaking structure with free space in the extended layer; (b) non-ideal ( $c=0.001$ ) cloaking structure with anticloak in the extended layer; (c) ideal ( $c=0$ ) cloaking structure with anticloak in the extended layer; (d) PEC cylinder with radius  $d$ . Five regions are apparent: (1) PEC cylinder; (2) extended layer; (3) cloaking shell; (4) free space; (5) scattered field region.

#### 4. ANALYTICAL MODEL

One important difference between time-domain and frequency-domain methods is that a time-domain method always gives a unique solution, while a frequency-domain method may have multiple solutions for a lossless case, given that the uniqueness theorem does not hold in general for a purely lossless case [22]. In order to justify uniqueness in a nondissipative media, infinitesimal losses are traditionally assumed. This treatment is realistic because losses are always unavoidable. In order to explain the physics behind the nonpenetration of electromagnetic waves through the interface between an ideal cloak and an ideal anticloak, we adopt a model similar to that of [6]. As depicted in Fig. 3, a plane wave is normally incident onto a double-layer medium composed of two regions, region 1 and region 2. The permittivity of the material in region 1 is  $\epsilon_1$ , while its permeability is  $\mu_1$ . The material of permittivity  $\epsilon_2$  and permeability  $\mu_2$ , in region 2 is obtained by the coordinate transformation  $x=-x'$ , which leads to  $\epsilon_2=-\epsilon_1$  and  $\mu_2=-\mu_1$ . From the transformation

theory point of view, region 2 is able to perfectly reconstruct the electromagnetic space in region 1 so that region 1 is cancelled by region 2 as if nothing were there. This property can be verified by straightforward calculations [15]. However, the materials at both sides of the cloak/anticloak interface have extreme values that may alter the effect of the cancellation. In agreement with the value of permittivity and permeability at the inner boundary of the cloak, we let  $\epsilon_1 \rightarrow +0$  and  $\mu_1 \rightarrow +\infty$  while their product

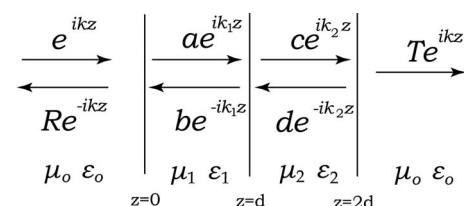


Fig. 3. Simple model illustrating why a normally incident wave cannot penetrate a slightly dispersive ideal cloak/anticloak double-layered slab.

remains constant, such that  $\varepsilon_1\mu_1=\varepsilon_0\mu_0$ . Consequently,  $\varepsilon_2\rightarrow -0$  and  $\mu_2\rightarrow -\infty$  while  $\varepsilon_2\mu_2=\varepsilon_0\mu_0$ . In order to represent the losses, a constant imaginary part is incorporated to the constitutive parameters: the permittivity and permeability in region 1 are now  $\varepsilon_1+i\delta$  and  $\mu_1+i\delta$ , respectively; those in region 2 are  $-\varepsilon_1+i\delta$  and  $-\mu_1+i\delta$ , respectively. Assuming that  $\varepsilon_1\rightarrow +0$  and  $\mu_1\rightarrow +\infty$ , the transmission coefficient is calculated behind the double-layer slab in Fig. 3. It is found that the transmission coefficient in this case is zero, indicating that the typical losses that are intrinsic to any material ensure that the electromagnetic wave cannot penetrate through the cloak/anticloak interface.

If the cloak is nondissipative and if  $c=0$ , the analysis presented in [5,15] cannot be carried out due to the singularity of the Hankel function at this point. Accordingly, the condition of conservation of the  $E$  and  $H$  fields's tangential components at  $r=R_1$  is degenerated, which leads to the conclusion that more than one solution is analytically possible. However, the lossless medium can be considered as the limit of the lossy medium as  $\delta\rightarrow 0$ . This statement is strengthened by the numerical results obtained above showing that a slight dissipation in the cloak material is of no consequence to the  $E$  field mapping depicted in Fig. 2(c). Thus, the uniqueness theorem holds and ensures that only one analytical solution is compatible with the physical limitation of loss. Though mathematically possible, the other ones do not represent the physical solution. In this sense, our numerical simulations clearly indicate that no field can penetrate the lossless cloak/anticloak boundary if  $\mu_\varphi$  is infinite.

## 5. CONCLUSION

We have extended and employed TLM to model a cylindrical cloak whose optic constants at the inner boundary take extreme values. The importance of assuming such extreme values in some conditions is illustrated by filling out the inner region of the cloak by an anisotropic material capable of destroying the cloaking effect. As shown by Chen *et al.* in their pioneering work, we have verified that the anticloak is effective for an almost perfect cloak. However, the ideal situation for which the optics constants take extreme values required further analysis. We have proven that TLM can efficiently model dielectric or magnetic constants tending to infinity, allowing the simulation of the ideal situation. The numerical results clearly show that the anticloak cannot defeat the cloaking phenomenon in the presence of an extreme layer, even if slight electric losses are incorporated into the material. With a simple analytical model, we have explained the result for a lossy medium: the lossless case following from the uniqueness theorem.

## ACKNOWLEDGMENTS

This work was partially supported by the Ministerio de Educación y Ciencia of Spain and Consejería de Innovación, Ciencia y Empresa of the Andalusian Government under projects FIS2007-63293 and PO7-FQM-03280, co-financed with FEDER funds of the European Union. H. Chen acknowledges the National Natural Science Foun-

dation of China (NNSFC) under grant 60801005, the Zhejiang Provincial Natural Science Foundation under grant R1080320, and the Ph.D. Programs Foundation of MEC under grant 200803351025. B. I. Wu acknowledges the Office of Naval Research (ONR) under contract N00014-06-1-0001 and the Department of the Air Force under contract FA8721-05-C-0002.

## REFERENCES

1. J. B. Pendry, D. Schurig, and D. R. Smith, "Controlling electromagnetic fields," *Science* **312**, 1780–1782 (2006).
2. D. Schurig, J. J. Mock, B. J. Justice, S. A. Cummer, J. B. Pendry, A. F. Starr, and D. R. Smith, "Metamaterial electromagnetic cloak at microwave frequencies," *Science* **314**, 977–980 (2006).
3. F. Zolla, S. Guenneau, A. Nicolet, and J. B. Pendry, "Electromagnetic analysis of cylindrical invisibility cloaks and the mirage effect," *Opt. Lett.* **32**, 1069–1071 (2007).
4. H. Chen, B.-I. Wu, B. Zhang, and J. A. Kong, "Electromagnetic wave interactions with a metamaterial cloak," *Phys. Rev. Lett.* **99**, 063903 (2007).
5. Z. Ruan, M. Yan, C. W. Neff, and M. Qiu, "Ideal cylindrical cloak: perfect but sensitive to tiny perturbations," *Phys. Rev. Lett.* **99**, 113903 (2007).
6. B. Zhang, H. Chen, B.-I. Wu, Y. Luo, L. Ran, and J. A. Kong, "Response of a cylindrical invisibility cloak to electromagnetic waves," *Phys. Rev. B* **76**, 121101(R) (2007).
7. H. Chen, Z. Liang, P. Yao, X. Jiang, H. Ma, and C. T. Chan, "Extending the bandwidth of electromagnetic cloaks," *Phys. Rev. B* **76**, 241104(R) (2007).
8. M. Yan, Z. Ruan, and M. Qiu, "Cylindrical invisibility cloak with simplified material parameters is inherently visible," *Phys. Rev. Lett.* **99**, 233901 (2007).
9. A. Nicolet, F. Zolla, and S. Guenneau, "Electromagnetic analysis of cylindrical cloaks of an arbitrary cross section," *Opt. Lett.* **33**, 1584–1586 (2008).
10. B. Zhang, H. Chen, B.-I. Wu, and J. A. Kong, "Extraordinary surface voltage effect in the invisibility cloak with an active device inside," *Phys. Rev. Lett.* **100**, 063904 (2008).
11. S. A. Cummer, B.-I. Popa, D. Schurig, D. R. Smith, and J. B. Pendry, "Full-wave simulations of electromagnetic cloaking structures," *Phys. Rev. E* **74**, 036621 (2006).
12. C. Blanchard, J. A. Portí, B.-I. Wu, J. A. Morente, A. Salinas, and J. A. Kong, "Time-domain simulation of electromagnetic cloaking structures with TLM method," *Opt. Express* **16**, 6461–6470 (2008).
13. Z. Liang, P. Yao, X. Sun, and X. Jiang, "The physical picture and the essential elements of the dynamical process for dispersive cloaking structures," *Appl. Phys. Lett.* **92**, 131118 (2008).
14. Y. Zhao, C. Argyropoulos, and Y. Hao, "Full-wave finite-difference time-domain simulation of electromagnetic cloaking structures," *Opt. Express* **16**, 6717–6730 (2008).
15. H. Chen, X. Luo, H. Ma, and C. T. Chan, "The anti-cloak," *Opt. Express* **16**, 14603–14608 (2008).
16. G. Castaldi, I. Gallina, V. Galdi, A. Alù, and N. Engheta, "Cloak/anticloak interactions," *Opt. Express* **17**, 3101–3114 (2009).
17. P. B. Johns and R. L. Beurle, "Numerical solution of 2-dimensional scattering problems using a transmission-line matrix," *Proc. Inst. Electr. Eng.* **118**, 1203–1208 (1971).
18. P. B. Johns, "A symmetrical condensed node for the TLM method," *IEEE Trans. Microwave Theory Tech.* **35**, 370–377 (1987).
19. J. A. Portí, J. A. Morente, A. Salinas, M. Rodríguez-Sola, and C. Blanchard, "On the circuit description of TLM nodes," *Int. J. Electron.* **93**, 479–491 (2006).

20. P. P. M. So, H. Du, and W. J. R. Hoefer, "Modeling of metamaterials with negative refractive index using 2-D shunt and 3-D SCN TLM networks," *IEEE Trans. Microwave Theory Tech.* **53**, 1496–1505 (2005).
21. C. Blanchard, J. A. Portí, J. A. Morente, A. Salinas, and B.-I. Wu, "Numerical determination of frequency behavior in cloaking structures based on L-C distributed networks with TLM method," *Opt. Express* **16**, 9344–9350 (2008).
22. C. A. Balanis, *Advanced Engineering Electromagnetics* (Wiley, 1989).